

Using multicarrier modulation in an ultrasonic data link to communicate with an underwater vehicle

**Eric T M Law¹, Robin Bradbeer¹, Lam F Yeung¹, Li Bin², Gu ZhongGuo²
and Tom H T Kwan¹**

¹ Department of Electronic Engineering, City University of Hong Kong, Hong Kong

² Institute of Acoustic Engineering, Northwestern Polytechnical University, Xi'an, 710072, China

Email: tmlaw@ee.cityu.edu.hk

Abstract:

Most current underwater remote operated vehicles (ROV) are controlled using data sent along an umbilical link to a base station. These umbilical cables cause problems with the control of the vehicle. This paper describes the prototype of an ultrasonic communications system that dispenses with the umbilical and uses an ultrasonic modem to transmit colour, still and video, pictures, as well as data, to and from such an ROV.

The system described in this paper uses Multicarrier Modulation, and has been successfully tested at a data rate up to 10kbps over 1km. The system algorithm generates 48 frequencies for transmitting 48 parallel bits of data in each packet. A long transmitted signal sequence is combined with synchronisation, zero gap and information packets. The long multi-frequency signal packets have been implemented to minimise the effect of multipath fading, which is a particular problem in shallow, open water environments. To acquire the starting point of the transmitting sequence, the Linear Frequency Modulation (LFM) signal is used for synchronisation. In order to reduce noise, the adaptive threshold packets are used to set up a suitable signal.

Various system architectures, such as the training pulse, channel identification etc are described. The equalisation and error correction can be added to reduce Intersymbol Interference (ISI) and error rate. The LMS algorithm is common for adaptive equaliser to adjust the tap coefficients. Reed-Solomon (RS) code will be used in the system to provide better image quality by reducing the bit error ratio.

Experimental results from sea-trials have shown that the system can cope with multipath fading environments.

Keywords: Multicarrier modulation, linear frequency modulation, Reed-Solomon code

1. Introduction

The main problem with using ultrasonic communication underwater is the complexity of the water channel. Channel imperfections are commonly numerous, being caused by water motion, density gradients, multi-paths, and the non-homogeneity of the water due to particles of solid or gaseous matter. Multi-paths can exist in almost any medium, whether bounded or unbounded. Reflections from boundaries can create signal paths between transmitter and receiver in addition to the direct path. In unbounded media, it is feasible that spurious signal paths may be created by temperature or velocity gradients. The effect of temperature gradients can be to refract a wave front such that the signal is bent round to the point of reception,

so, interfering with the direct signal. Similarly a velocity gradient lying across the axis of wave propagation can cause what appears to be refraction, bending the wave front. In a shallow, open water environment, the multipath problem is mainly due to reflections from the surface of the water and the sea or lake floor. Previous work at City University of Hong Kong [1 - 4] has shown that it is possible to send data reliably through liquid filled pipes, where the multipath problem is considerable.

As mentioned by Poor and Wornell [5], there are three methods of underwater acoustic communication systems. The first is a 'no diversity' technique; the second is 'only explicit

diversity reception' such as time, frequency diversity etc; the third is 'at least implicit diversity' processing. This method spectrally spreads the signal over a single transmission band so that bandwidth is much larger than the coherence bandwidth of channel.

The first method of underwater acoustic communication systems uses a no diversity technique so that it can implement the system easily. However, it has low data rate and reliability over a short range because of the multipath fading problem. The second method

uses explicit diversity reception. The advantage of this system is a higher data rate and reliability with longer transmission range. But its complexity and power consumption are also increased. The third method uses 'at least implicit' diversity reception. As described by Poor and Wornell [5], it can provide the highest reliability, speed and power efficiency, but it requires the most complex system to implement.

In the following table, different methods are shown based on current experimental results.

Developed by	Water depth (m)	Carrier frequency (Hz)	Distance (km)	Modulation	Data rate (bps)
Stojanovic et al. [6]	100-200	25k	3	QPSK	10k
Freitag and Catipovic [7]	6-18	25k	0.7	MFSK	5k
Catipovic and Freitag [8]	6-20	20k	0.75	128-FSK	10k
Yeo et al. [9]	~ 18	10k	5 (maximum)	QPSK / BPSK	4k
Leinhos [10]	~ 40 feet	3.5k	~ 6.5 knots	1870-coded QPSK	1250 symbols per second

Table 1. Existing results of underwater acoustic communication

In this paper, we describe the multicarrier modulation system with a data rate 10kbps over 1km which using 48 frequencies in 43k to 53k Hz. Section 2 describes the structure of data sequence. Synchronisation and multicarrier modulation are described in section 3 and 4 respectively. Section 5 mentions channel identification. System configuration is discussed in section 6. Section 7 and 8 discuss equalisation method and error correction respectively. Experimental results are described in section 9.

2. Data Sequence

The data sequence is in packet form. The sequence contains synchronisation packets, gap packet, adaptive threshold packets and information data packets. These packets are used to allow synchronisation and noise reduction. Each packet is formed by 48 frequencies within 43kHz to 53kHz, which represent 48 bits with a duration of 5.12ms.

The sequence begins with the Linear Frequency Modulation (LFM) signal packet which is used to synchronise the receiver to the start of the data. The details of LFM signal will be discussed in the next section. Then a packet of the gap signal follows the LFM packet so that synchronisation can be performed in this period. Eight adaptive threshold packets (ATP) are transmitted for receiver-training purposes. The training packets act as a reference of the transmitted signal block so that channel estimation can be calculated from the reference packets. Also, the long training sequence can be sufficient for the system convergence. 800 information data packets (IDP) follow the adaptive packets. At the end of the data sequence, is also a gap signal packet which can minimise the effect of multipath fading between two signal blocks. The time duration for one signal block is $(1+1+8+800+1)*5.12ms = 4.15s$. Fig. 1 shows the data sequence.

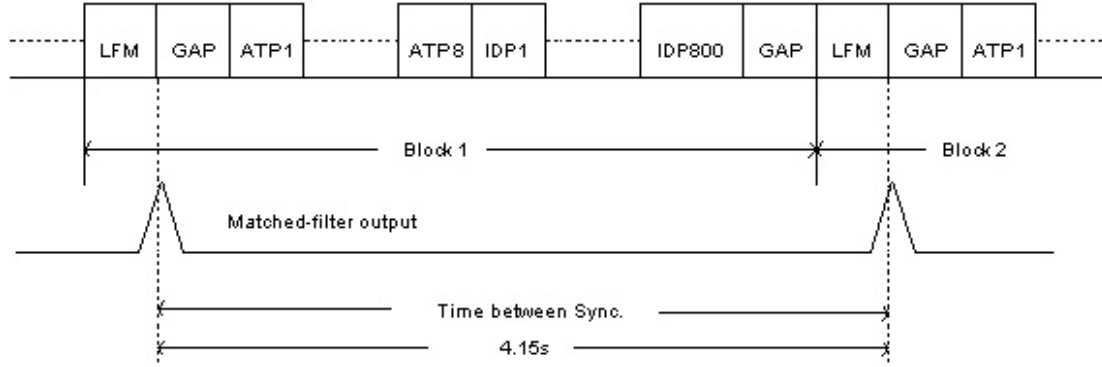


Fig. 1. Data Structure with LFM signal for synchronisation

3. Synchronisation

For many current systems, a Linear Frequency Modulation (LFM) signal is used for frame synchronisation. The most significant property of the linear frequency modulation signal is its symmetry in time and frequency. In general, the expression for a linear frequency modulation signal, also referred to as a ‘chirp’ is mentioned by Rihazek [11] as:

$$s(t) = \cos(2\pi f_0 t + \pi k t^2) \quad (1)$$

The instantaneous frequency can be obtained by differentiation

$$f(t) = \frac{1}{2\pi} \cdot \frac{d}{dt}(2\pi f_0 t + \pi k t^2) = f_0 + k t \quad (2)$$

where f_0 is initial frequency, $|k| = \frac{B}{T}$, B is the

bandwidth and T is the signal duration. Hence the LFM chirp described by Rihazek [11] is characterised by its starting frequency (f_0), stopping frequency (f_1), and time duration (T) as:

$$|k| = \frac{|f_1 - f_0|}{T} = \frac{B}{T} \quad (3)$$

The resolution of the time depends on the BT product.

At the receiver, a matched-filter is used to indicate the arrival of the LFM chirp. The output of this correlation allows selection of the channel with the most energy for synchronisation. The impulse-like auto-correlation function of the LFM signal in Fig.2 allows synchronisation to be achieved by linear cross-correlation between the received signal and a known LFM signal. Therefore, the starting position of the data sequence can be found by output of the matched-filter.

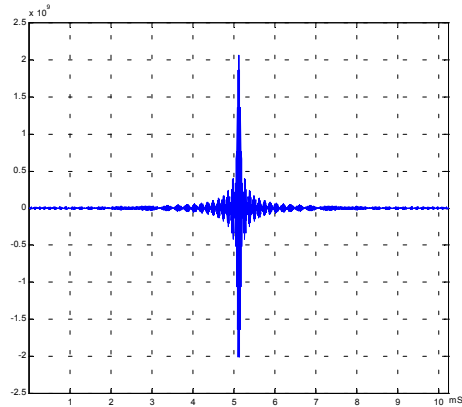


Fig. 2. Ideal output of the matched-filter of the synchronisation signal

4. Multicarrier Modulation

Multicarrier modulation divides a channel into a set of parallel independent subchannels [14]. The SNR of each subchannel is measured and a suitable number of bits is then assigned to each channel. There are two reasons for choosing Multicarrier Modulation (MCM) in the system. According to Bingham [12], the MCM signal can be processed in a receiver without the enhancement of noise or interference that is caused by linear equalisation of a single-carrier signal. Another is that the long symbol time used in MCM produces a much greater immunity to impulse noise and fast fades. According to Bingham [12] and Proakis [13], the input data is Mf_s b/s. They are grouped into blocks of M bits at block (symbol) rate of f_s . Therefore

$$f_{c,n} = n\Delta f \quad \text{for } n = n_1 \text{ to } n_2 \quad (4)$$

$$M = \sum_{n=n_1}^{n_2} m_n \quad (5)$$

where $N_c = n_2 - n_1 + 1$, $f_{c,n}$ = carrier frequency, Δf = frequency separation and

N_c = number of carriers.

$$\hat{H}_n = \frac{1}{L} \sum_{i=1}^L \frac{Y_{i,n}}{X_n} \quad (8)$$

$$y_n = |H_n| x_n + n_n \quad (9)$$

In our system, the modulation and demodulation techniques used are IFFT and FFT. IFFT and FFT are well-known efficient algorithms and significantly reduce the complexity of implementing the modulation and demodulation functions. The benefit in system implementation using IFFT and FFT are mentioned by Lee et al. [14] Rizos et al. [15]. However, the resulting signalling filters have relatively large overlapping sidelobes (-13dB), and this causes a deviation from the ideal multicarrier scheme of independent carriers.

In our system, the binary input data are parsed to each subchannel with fixed number of bits for system initialisation. The number of bits for each subchannel is determined by measuring the SNR of each subchannel during startup. As our system is half-duplex there is no feedback signal back to the transmitter. Therefore a fixed number of bits is used instead of varying bit numbers. Details will be discussed in section 6.

Mathematically, the discrete complex multicarrier modulation signal [16] can be represented for n^{th} sample by:

$$s(nT) = \frac{1}{N} \sum_{k=0}^{N-1} A_k e^{j(2n\pi f_k T + \phi_k)} \quad (6)$$

The sampling frequency is $1/T$ and the period of one data symbol is $2NT$ with inter-modulation frequency domain. The frequency, f_k , is given by:

$$f_k = f_0 + k(\Delta f) \quad (7)$$

where f_0 is the lowest frequency of the signal spectrum and $\Delta f = 1/NT$ is the frequency separation between carriers.

5. Channel Identification

As mentioned by Lee et al. [14] Chow et al. [17], a periodic training sequence x_k with period M is needed once for every transmitted block of bits which is equal to or slightly larger than the length of the channel pulse response. The receiver measures the corresponding channel output averaging over L cycles, and then divides the FFT of the channel output by the FFT of the known training sequence. The channel estimate in the frequency domain is

where $Y_{i,n}$ is the n^{th} element of the FFT of the channel output on i^{th} cycle and X_n is the n^{th} element of the FFT of the input training sequence. x_n and y_n are input training sequence and channel output in time-domain respectively. n_n is noise in n^{th} element. $H_n = h_0 + h_1 e^{-j(2\pi/N)n} + h_2 e^{-j(2\pi/N)n} + \dots + h_v e^{-j(2\pi/N)vn}$

6. System Configuration

Fig. 3 shows a block diagram of the system. In the transmitter, a serial-to-parallel (s/p) buffer, adaptive threshold packets, MFSK modulator, LFM signal packet and parallel-to-serial (p/s) buffer are generated by a DSP TMS320C542. Also synchronisation, s/p and p/s buffers, MFSK demodulator and threshold learning are performed by a DSP unit in the receiver.

In the transmitter, the input data is first transmitted from a PC to the Underwater Acoustic Modem via an RS232 link. The data is then converted from serial to parallel form by a serial-to-parallel buffer. The binary input data are parsed to each subchannel with one bit. Therefore there are 48 parallel bits represented by 48 frequency components, so the parallel data bits can be modulated by multicarrier modulation.

To overcome the multipath fading, eight adaptive threshold packets are added at the front of input data sequence before transmission. Each packet contains 48 bits. The odd packets are [101010...101010] and even packets are [010101...010101]. This is used as a reference signal for the receiver to estimate the channel, and then the IFFT algorithm is used for modulation.

As mentioned above, there are 48 frequency components within 43kHz to 53kHz. They are equally distributed in the frequency range, so that the frequency separation between carriers is $\Delta f = \frac{53k - 43k}{48} \approx 200\text{Hz}$. The choice of number of carriers is determined by the implementation in the DSP. The TMS320C542 is a 16 bits (one word) fixed point DSP, so that multiples of 16 bits are used due to easy

implementation. In the system, 48 bits (3 words) are used for each data packet. [8] Also, the choice of the number of tones is a trade-off between the system sensitivity to multipath and practical implementation constraints.

After IFFT modulation, the data is converted from the frequency to time domain. At that time, the LFM signal is implemented at the front time slot of the data sequence. This is used for synchronisation in receiver.

In the receiver, some of the noise is reduced using a bandpass filter of 40kHz to 60kHz. The matched-filter captures the LFM signal from the received signal, which indicates the start of the data sequence. The output of this correlation provides an estimation of the channel that is used to select the pulse with the most energy for synchronisation. Then the data sequence is demodulated by the FFT algorithm. The data packets are converted from the time-domain to frequency-domain so that decoding can be take place in the error correction algorithm.

Once synchronisation has been achieved, threshold learning can be used to calculate the channel characteristic. Because the acoustic channel is a time varying channel, a fixed threshold cannot work well in the system. Therefore, the threshold of the detector is changed by transmitted reference packets at each data sequence. These change every 4.15s of the data sequence. Adaptive threshold in frequency-domain is used and the training signal is sent out repeatedly after each time the LFM signal was send. At the receiver, the frequency-domain's threshold is calculated from the known training signal and the received training signal. According to the received training signal's frequency-domain characteristic, the adaptive threshold is calculated. This can be used to estimate the channel characteristic. [8] Depending on the acoustic channel, an equaliser/echo canceller may be inserted into system at this point; otherwise the output of the FFT is passed to an error-correction algorithm.

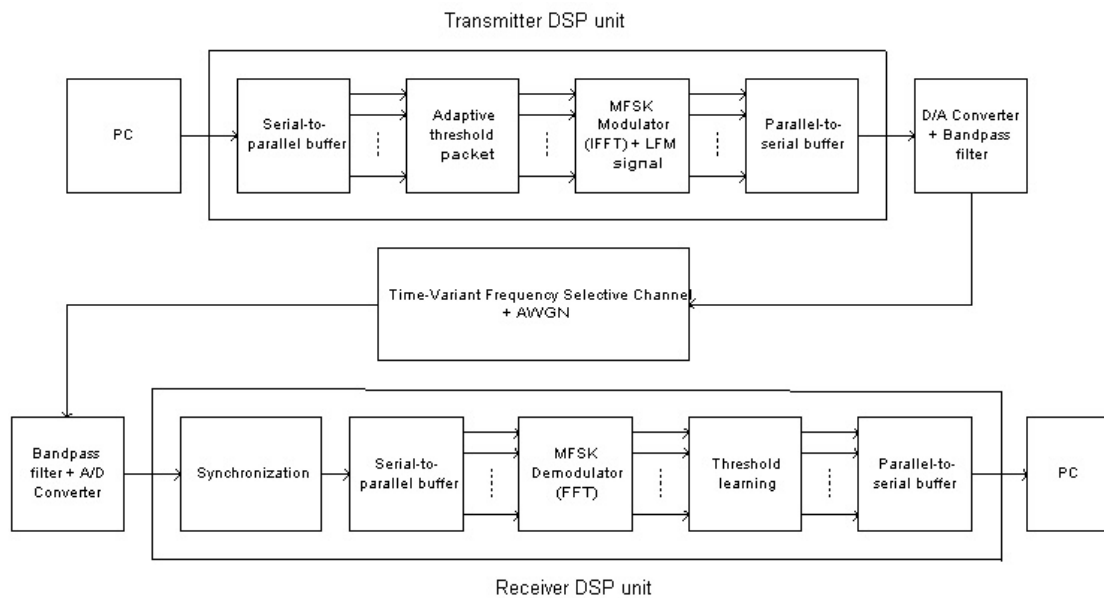


Fig. 3. System Configuration

7. Equalisation

Due to the unknown time-invariant channel, intersymbol interference (ISI) may occur. So a channel equaliser is used to reduce ISI. The adaptive equaliser updates its parameters in each period during the data transmission. The adaptive equaliser must track time variants in the channel response and adapt its coefficients to reduce ISI. In this case, LMS algorithm has been used.

As mentioned by Proakis [13], the equaliser tap coefficients may be expressed as

$$\hat{C}_{k+1} = \hat{C}_k - \Delta \hat{G}_k \quad (10)$$

where \hat{C}_k and \hat{G}_k are estimated tap vector coefficients and estimated gradient vector respectively.

$$\therefore \hat{G}_k = -\varepsilon_k V_k^* \quad (11)$$

$$\therefore \hat{C}_{k+1} = \hat{C}_k + \Delta \varepsilon_k V_k^* \quad (12)$$

The vector \hat{C}_k represents the set of coefficients at the k th iteration, $\varepsilon_k = I_k - \hat{I}_k$ is the error signal at the k th iteration, V_k is the vector of received signal samples that make up the estimate \hat{I}_k , i.e., $V_k = [v_{k+K} \cdots v_k \cdots v_{k-K}]^T$, and Δ is a positive number chosen small enough to ensure convergence of the iterative procedure.

It has assumed that the knowledge of the transmitted signal has been known in the receiver so that the error signal can be calculated from the desired symbol and its estimated symbol. A short training period with known information sequence is transmitted to adjust the tap coefficients initially. After the initial adjustment, the adaptive equaliser switches to decision-directed mode. In this case the decision of the output detector depends on error signal which is formed by the difference between decision output of the receiver and estimated output.

8. Error Correction

To reduce the error rate, information should be protected by parity checking bytes. A number of error control coding schemes are available and Reed-Solomon (RS) code is the most suitable for incorporating in the Underwater Acoustic Modem (UAM) for the following reasons:

- RS is well known for combating burst error which is an obvious characteristic of the UAM error pattern

- The parameters of RS (n, k, t) can be varied to compromise with various error rate and data rate requirements.
- There is plenty of software and hardware for RS implementation.

Reed-Solomon code is bounded by the following parameters [19]:

$$\text{Block Length} \quad n = q^m - 1$$

$$\text{Number of Parity-check Digits} \quad 2t = n - k$$

$$\text{Minimum Distance} \quad d_{\min} = 2t + 1$$

Encoding of RS is by multiplying the information polynomial with the generator polynomial $g(x)$:

$$g(x) = (x + \alpha)(x + \alpha^2) \cdots (x + \alpha^{2t}) \quad (13)$$

The decoding of RS is more complicated involving 4 steps [19]

1. Syndrome Computation [18]
2. The Berlekamp Massey Algorithm [18] for finding the error locator polynomial
3. The Chien Search Algorithm [18] for solving for the root of the error locator polynomial
4. The Forney algorithm [18] for computing the error magnitudes

There are 2 approaches to implementation

1. By inserting hardware chip sets for RS encoding and decoding.

This is an easy way of implementation, however inserting chipset increases the complexity of the circuit and might cause more noise in the signals.

2. By embedding the encoding and decoding in the DSP program of the transmitter and receiver.

This is a much more economic choice and the flexibility is much higher. However the complexity of the decoding process usually requires high speed processor and long software development time.

The latter choice is more preferable since there are processors in the market which are empowered with special instructions for finite field arithmetic operations. Such instruction sets reduce the computational complexity of the decoding process.

The following is the performance of RS decoding programs using the TMS320C64x processor. The RS code uses a shortened code word of (204, 188) which can correct up to 8 error symbols. The following table [18] describes the performance of RS code.

Name of Module	C Code	Assembly Optimizer	Hand Optimized
Syndrome Accumulate	480 cycles	470 cycles	470 cycles
Chien Search	1110 cycles	326 cycles	318 cycles
Berlekamp-Massey	340 cycles	263 cycles	246 cycles
Forney	180 cycles	154 cycles	150 cycles
Driver Function	80 cycles	80 cycles	80 cycles
Reed Solomon Decoder	2180 cycles	1293 cycles	1268 cycles

Table 2: RS performance (Taken from [18])

9. Experimental Results

The system has been tested in CityU's swimming pool and in coastal area near Hong Kong. The pool has dimensions of 50m x 25m, and the transducers are at a depth of 0.6m. Fig. 4a shows the synchronisation signal and Fig. 4b is the signal after the matched-filter. In Fig. 4b, there is serious multipath fading problem, and the reflected signals from the side walls and the bottom of the pool can be seen. Fig. 5 shows the results of sending a raw bit-mapped signal of 24 bits 80*60 pixels. The left hand picture is the sent signal. The others are from the received signal.

A number of open water sea trials have also been carried out. One took place at Da Mei Do, in the New Territories of Hong Kong. The geographic environment is shown in Fig. 6. Two transducers are at a depth of 4 metres. The receiver is at the wharf and the transmitter on the boat. The depth of the water is 5.6 metres at the wharf and the 8 metres deep at the boat. The distance between two transducers is 820m, measured by GPS. Fig. 7 shows the received pictures using the same sent signal as in Fig. 5. The error rate of the raw data is less than 5%.

10. Conclusion

In this paper, a multicarrier modulation underwater acoustic system has been developed and demonstrated the ability of real time underwater acoustic communication. The system performed at a data rate of 10kbps over 1km.

Current work in developing the system involves using error correction techniques, adaptive filtering to achieve a higher data rate and reliability. The error rate can also be improved by implementing channel equalisation and channel coding.

The turbo equalisation and turbo coding will be implemented to get higher data rate with higher reliability. Due to the effect of multipath fading, varies code lengths of turbo code will be investigated to find the optimum code length in our future analysis.

11. Acknowledgments

This work has been supported by This work is supported by City University of Hong Kong Grants 7001137 and 9410007.

12. Reference

- [1] Liao, D Z; Harrold, S O; Yeung, L F, "An underwater Acoustic Data Link for Autonomous Underwater Vehicles", IEEE Int. Conf. in Circuit and Systems, p28-33, Singapore, July 1995.
- [2] Harrold, S O; Liao, D Z; Yeung, L F, "Ultrasonic Data Communication Along Large Diameter Water-filled Pipes", IEEE Int. Conf. M²VIP, Hong Kong, 1996.
- [3] Yinghui Li; Harrold, S O; Yeung, L F, "Experimental Study On Ultrasonic Signal Transmission With The Water-Filled Pipes", IEEE Int. Conf. M²VIP, Sept 1997, Australia.
- [4] Li Bin; Harrold, S O; Bradbeer, R; Yeung, L F, "An Underwater Acoustic Digital Communication Link", in *Mechatronics and Machine Vision*, (J Billingsley (Ed)), Research Studies Press, UK, pp 275-282, 2000
- [5] H. V. Poor and G. W. Wornell, *Wireless Communications: Signal Processing Perspectives*, New Jersey, Prentice-Hall, Inc, 1998, pp.353-356.
- [6] M. Stojanovic, L. Freitag and M. Johnson, "Channel-Estimation-Based Adaptive Equalization of Underwater Acoustic Signals", OCEANS '99 MTS/IEEE, Riding the Crest into the 21st Century, vol.2, 1999, pp.985-990.
- [7] L. E. Freitag and J. A. Catipovic, "A Signal Processing System for Underwater Acoustic ROV Communication", Proceedings of the 6th International Symposium on Unmanned Untethered Submersible Technology, 1989, pp.34-41.
- [8] J. A. Catipovic and L. E. Freitag, "High Data Rate Acoustic Telemetry for Moving ROVS in a Fading Multipath Shallow Water Environment", Proceedings of the Symposium on Autonomous Underwater Vehicle Technology, 1990, pp.296-303.
- [9] H. K. Yeo, B. S. Sharif, A. E. Adams and O. R. Hinton, "Multiuser Detection for Time-Variant Multipath Environment", Proceedings of the 2000 International Symposium on Underwater Technology, 2000, pp.399-404.
- [10] H. A. Leinhos, "Block-Adaptive Decision Feedback Equalization with Integral Error Correction for Underwater Acoustic Communications", OCEANS 2000 MTS/IEEE Conference and Exhibition, vol.2, 2000, pp.817-822.
- [11] A. W. Rihazek, *Principles of High-Resolution Radar*, Peninsula Publishing, 1985, pp.226-231.
- [12] J.A.C. Bingham, 'Multicarrier Modulation for Data Transmission: An Idea Whose Time Has Come', IEEE Communications Magazine, 1990, pp.5-14.
- [13] J. G. Proakis, *Digital Communication*, 3rd Edition, McGraw-Hill, Inc, New York, 1995.
- [14] I. Lee, J.S. Chow and J.M. Cioffi, 'Performance Evaluation of a Fast Computation Algorithm for the DMT in High-Speed Subscriber Loop', IEEE Journal on Selected Areas in Communications, 1995, pp.1564-1570.
- [15] A.D. Rizos, J.G. Proakis and T.Q. Nguyen, 'Comparison of DFT and Cosine Modulated Filter Banks in Multicarrier Modulation', IEEE Global Telecommunications Conference, 1994, pp.687-691.
- [16] W. K. Lam and R. F. Ormondroyd, "A Coherent COFDM Modulation System for A Time-Varying Frequency-Selective Underwater Acoustic Channel", 7th International Conference on Electronic Engineering in Oceanography, 23-25 June 1997, pp.198-203.
- [17] J.S. Chow, J.C. Tu and J.M. Cioffi, 'A Discrete Multitone Transceiver System for HDSL Applications', IEEE Journal on Selected Areas in Communications, 1991, pp.895-908.
- [18] J. Sankaran, Reed Solomon Decoder: TMS320C64x Implementation, SPRA686 – Dec. 2000.
- [19] S. B. Wicker, V. K. Bhargava, *Reed Solomon Codes and Their Applications*, IEEE Press, N.J., 1994.